

# Enhancing PRNU-based image forensics with a non-parametric correlation predictor based on Locally Weighted Regression

**Sujoy Chakraborty and Erick Garcia-Vargas**  
Department of Computer Science, Stockton University  
Galloway, NJ/USA

## Abstract

*For PRNU-based image manipulation localization, the correlation predictor plays a crucial role to reduce false positives considerably, as well as increasing accuracy of manipulation localization. In this paper, we propose a novel correlation predictor with a non-parametric learning algorithm, which is Locally Weighted Regression. Instead of fitting a global set of model parameters, a non-parametric learning algorithm fits a model dynamically by sampling the training set based on the pixel in the query image at which the correlation needs to be predicted. Our experimental results suggest that building a model dynamically based on the distance of training examples from the query pixel in the feature space helps to predict the correlation more accurately. Experimental results on benchmark datasets indicate that integrating the new predictor significantly improves the accuracy of predicted correlation, as well as image manipulation localization performance of PRNU-based forensic detectors.*

## Introduction

For forensic analysis of digital images, the Photo-Response Non-Uniformity (PRNU) noise has been embraced by the forensic researchers as the most valuable characteristics [1], both for the forensic tasks of source attribution (camera identification) and manipulation localization. Minute material imperfections and manufacturing inconsistencies of the sensing elements of a camera gives rise to this unique spatially varying noise pattern, which is present as a fingerprint in every image captured by a digital camera [3]. This is particularly useful for device identification [4–10, 15, 17], which is the task of attributing a digital content (e.g., an image or a video) to the device used to capture it. It is a problem deeply investigated in forensic research and is useful to fight copyright infringement or distribution of illicit materials (terrorist threats, under-age clips etc.). Another key forensic application is to localize manipulations in digital images. When a copy-move or splicing manipulation is applied to an image, the manipulation operation distorts the fingerprint that was originally present in that region. A fundamental manipulation detector analyzes the query image in small analysis windows and compares the local noise estimate with the corresponding block in the camera PRNU in terms of a correlation score. A correlation value below a suitably chosen threshold indicates a potential manipulation. In recent times, more sophisticated detectors have been proposed that takes into account the neighborhood dependency of pixels for better accuracy of manipulation localization [11–14].

However, the fundamental problem with adapting a PRNU-based manipulation detector is that the value of the normalized correlation also depends on the content. Dark, textured and satu-

rated regions in an image are likely to yield a low correlation score even in the absence of a manipulation. As a remedy to this problem, a correlation predictor has been proposed [15], which predicts the expected value of the correlation depending upon the texture, intensity and flatness characteristics of an image, assuming the content to be genuine. If the predicted correlation is low, typically below some pre-determined threshold, a conservative decision is made for the corresponding analysis window. Therefore, to ensure low false positives and improve accuracy of manipulation localization, it is of paramount importance to integrate an adequate correlation predictor with the PRNU-based detectors. A more sophisticated correlation predictor would greatly enhance the performance of PRNU-based detectors proposed in the literature [11–14]. The classical correlation predictor proposed by Chen et. al. [15] is a least square fit to features representing texture, intensity and flatness characteristics in an image and the quadratic terms involving those features. A feed-forward neural network with features representing intensity, texture and flatness was used by Korus and Huang [12]. Recently, a deep learning approach was proposed by the author of this manuscript [16], where a Convolutional Neural Network (CNN) was allowed to automatically learn features for predicting the correlation score in a typical manipulation localization scenario.

In this paper, we propose a non-parametric approach towards predicting correlations for PRNU-based image forensics. The classical correlation predictor [15] learns a model based on the entire training set consisting of features representing texture, intensity and flatness characteristics and corresponding correlation values, for genuine image patches in the training set. Once the training is complete, the correlation score at a new pixel is computed by plugging in the feature values for the analysis window centering the query pixel in the learnt model. The prediction accuracy thus largely depends on the choice of the training set, as well as the predictor features in the analysis window of the query pixel. We propose a correlation predictor with Locally Weighted Regression, which is a non-parametric learning algorithm. With Locally Weighted Regression, we dynamically build a model from a subset of patches from the training set, which lie in the vicinity of the query pixel in the feature space. This ensures that analysis windows which are similar to that of the query pixel alone are considered when we build the model, leaving out points in the feature space that are far apart, thus ensuring high prediction accuracy. This work sets out to investigate the performance of PRNU-based manipulation localization when the proposed correlation predictor is integrated with PRNU-based manipulation detectors. Before we elaborate on the technical aspects of the proposed approach, we do a literature review of PRNU-based image forensics in gen-

eral in the next section. Subsequently, we present the proposed correlation predictor and discuss its advantages over the classical correlation predictor. In the following sections, we corroborate our technical findings with experimental results. Finally we draw our conclusions and discuss future research directions.

## Sensor-based image forensics

The camera sensor noise or the fingerprint of a camera can be estimated from a set of genuine sensor outputs  $x_1, x_2, \dots, x_L$ . We assume a multiplicative noise model and denote the ideal sensor output (in absence of noise) by  $\tilde{x}$  and the actual sensor output by  $x$ . Under this assumption, the sensor output captured by the device can be expressed as:

$$x = (1 + K) \cdot \tilde{x} + \theta. \quad (1)$$

Here,  $K$  is the fingerprint or PRNU of the camera and the modeling noise  $\theta$  is assumed to be I.I.D Gaussian. The Maximum Likelihood Estimate of the PRNU factor  $K$  is given by:

$$\hat{K} = \left( \sum_{l=1}^L \mathbf{w}_l \mathbf{x}_l \right) \cdot \left( \sum_{l=1}^L \mathbf{x}_l^2 \right)^{-1}, \quad (2)$$

where,  $\mathbf{w}_l = \mathbf{x}_l - F(\mathbf{x}_l)$  is the noise residual, or the sensor noise obtained by feeding image  $\mathbf{x}_l$  to a de-noising filter. A post-processing step is often applied to eliminate non-unique artifacts from lens distortion correction or demosaicing [3, 17].

The task of manipulation localization can be viewed as a statistical hypothesis testing problem, where a query image is inspected in small overlapping analysis windows centering every pixel, for the presence or absence of the camera fingerprint in the local noise estimate:

$$\begin{cases} H_0 : \mathbf{w} = \mathbf{x} - F(\mathbf{x}) \text{ does not contain the PRNU factor } \mathbf{K} \\ H_1 : \mathbf{w} \text{ contains the PRNU factor } \mathbf{K} \end{cases}$$

where,  $\mathbf{w}$  is the noise residue extracted from the analysis window.  $H_0$  is the null hypothesis which represents that the block under analysis is manipulated and hence doesn't contain the camera PRNU. The hypothesis  $H_1$  is the alternative hypothesis and represents the fact that the block under analysis is genuine and hence indeed contains the camera fingerprint. The hypothesis test can be decided in favor of  $H_0$  or  $H_1$  based on a computed correlation statistic and comparing the same to a predetermined threshold  $\tau$ :

$$\rho = \text{corr}(\mathbf{w}, (\mathbf{x}\hat{K})). \quad (3)$$

where, the standard algorithm decides for  $H_1$  if  $\rho > \tau$  and for  $H_0$  otherwise.

However, the fundamental correlation-based manipulation detector is inherently limited by the fact that the measured correlation depends on the content. If the content under analysis is of low intensity, or has texture or saturated pixels, then the correlation score would be low even if the content is genuine. Thus, to avoid declaring a genuine analysis window as manipulated and reduce false positives, a correlation predictor has been proposed [15], which predicts the correlation score that we expect to observe assuming the content to be genuine, based on the nature of content alone.

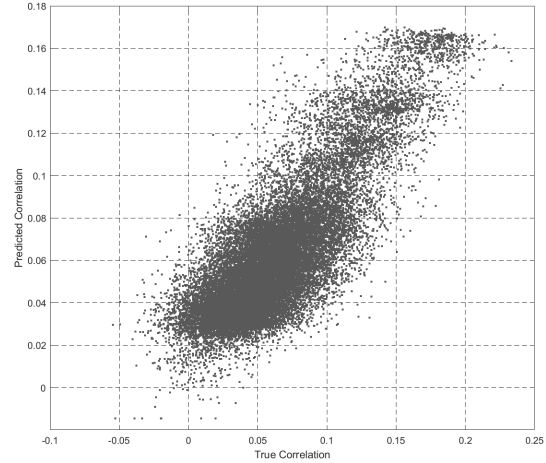


Figure 1: A typical scatter plot of predicted correlation vs. actual correlation.

The correlation predictor proposed by Chen et. al. [15] is a least square fit to features representing intensity, texture and flatness characteristics of the content under analysis. In the following subsection, we describe the correlation predictor and its application in a forensic scenario of manipulation localization.

## Correlation Predictor

The correlation predictor can be viewed as a mapping from a feature space to a real number, where the feature space consists of features representing the texture, intensity and flatness characteristics of the content. In forensic literature, the correlation predictor has been expressed as a linear combination of features quantifying the texture, intensity and flatness of the content under analysis [15]. What follows is a brief description of features used in the classical correlation predictor.

### Image intensity

Due to the fact that the PRNU term  $x\hat{K}$  is multiplicative, the correlation is typically high in regions of high intensity. However, the PRNU term is absent in saturated pixels (where we have  $x_i = 255$ , where  $x_i$  represents the  $i$ -th pixel in the image) and hence is attenuated over some critical intensity value  $\gamma$  ( $\gamma \leq x_i \leq 255$ ). The critical value of intensity  $\gamma$  depends on the camera. The intensity feature is defined as the average intensity attenuated close to the maximum dynamic range:

$$f_I = \frac{1}{|B|} \sum_{i \in B} att(x_i), \quad (4)$$

where  $|B|$  denotes the number of pixels in the image block under analysis. The attenuation function  $att(x)$  is defined as:

$$att(x) = \begin{cases} \exp(-(x - \gamma)^2 / \delta) & \text{if } x > \gamma \\ x/\gamma & \text{if } x \leq \gamma. \end{cases} \quad (5)$$

The parameters  $\gamma$  and  $\delta$  vary for different camera models.

### Texture

The correlation observed is typically low if the analysis window has textured content. Typically, the textured regions cor-

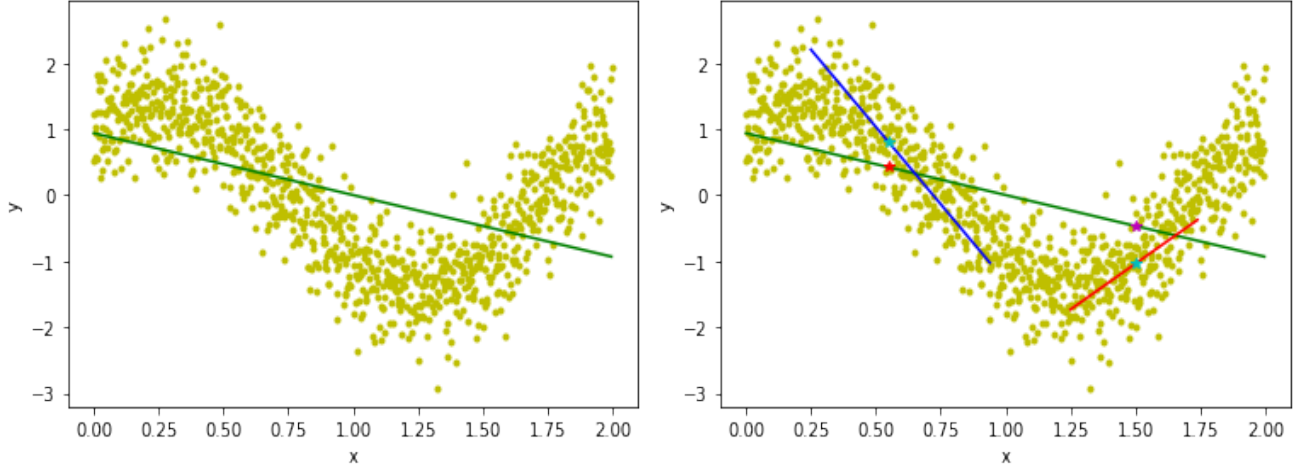


Figure 2: Comparing Linear Regression with Locally Weighted Regression. Left: Linear Regression fits a global set of parameters to the training set. Right: Locally Weighted Regression dynamically builds a model considering only the training examples that lie in the vicinity of the query point.

respond to high frequency and due to imperfect filtering, some traces of the textured content is also present along with the noise residual. This weakens the PRNU signal, which is essentially the signal of interest for manipulation localization. The texture feature is defined as:

$$f_T = \frac{1}{|B|} \sum_{i \in B} \frac{1}{1 + \sigma_i^2}, \quad (6)$$

where,  $\sigma_i$  denotes the standard deviation of the image intensity in a  $5 \times 5$  square block centering the  $i$ -th pixel in the analysis window  $B$  of the corresponding high-pass filtered image.

### Signal flattening

The predictor would overestimate the correlation score in a flat and unsaturated region in the image. Typically, such areas have a low variance of intensity. The signal flattening feature is defined as the ratio of pixels in the analysis window, with average intensity below a threshold:

$$f_S = \frac{1}{|B|} |\{i \in B, \sigma_i < \eta x_i\}|, \quad (7)$$

where,  $\eta$  is a constant that depends on the variance of the PRNU factor  $K$  and  $\sigma_i$  is the intensity variance of the analysis window centering the  $i$ -th pixel, measured from a  $5 \times 5$  neighborhood.

### Texture-Intensity

The correlation score is also dependent on the collective influence of intensity and texture (sometimes textured regions are also high-intensity regions). Thus, the texture-intensity feature has been defined to measure the combined effect of intensity and texture in the analysis window:

$$f_{TI} = \frac{1}{|B|} \sum_{i \in B} \frac{att(x_i)}{1 + \sigma_i^2}, \quad (8)$$

where,  $\sigma_i$  has the same definition as the corresponding term in the texture feature and the attenuation function has the same definition as that of the intensity feature in eq. (5).

With the features defined as above, the correlation predictor has been defined as simple polynomial multivariate model, where the coefficients of the model can be obtained by least-squares regression. If we have a training set consisting of  $m$  training examples (i.e., the feature values for  $m$  analysis windows and corresponding correlation values), then the correlation can be modeled as:

$$\rho[k] = \theta_0 + \theta_1 f_I[k] + \theta_2 f_T[k] + \theta_3 f_S[k] + \theta_4 f_{TI}[k] + \theta_5 f_I^2[k] + \theta_6 f_I[k] \cdot f_T[k] + \dots + \psi[k], \quad (9)$$

where,  $\psi$  is the modeling noise and  $\theta$  is the vector of coefficients to be determined,  $\theta \in \mathbb{R}^{15}$ . The above equation can be expressed in matrix-vector form as:

$$\rho = H\theta + \psi, \quad (10)$$

where,  $H$  is a matrix of dimension  $m \times 15$  and  $\theta = (\theta_0, \theta_1, \dots, \theta_{14})^T$  is the vector of parameters to be estimated. From Linear regression with least-squares fit, we have:

$$\hat{\theta} = (H^T H)^{-1} H^T \rho. \quad (11)$$

The estimate of coefficient vector  $\hat{\theta}$  is then used to predict the correlation from the measured features on a given analysis window:

$$\hat{\rho} = H\hat{\theta}. \quad (12)$$

Fig. 1 shows the scatter plot of predicted vs. measured correlation for a typical consumer digital camera.

### Locally Weighted Regression

The least-squares regression solution as given in eq. (11) fits a global set of parameters for the given training set. Thus, the parameters set will largely depend on the choice of the training set. Typically, the features can vary to a significant extent for different image patches and a linear regression model with quadratic terms might not always be a good fit. Hence, for a given query pixel for which the correlation needs to be predicted, a global set of

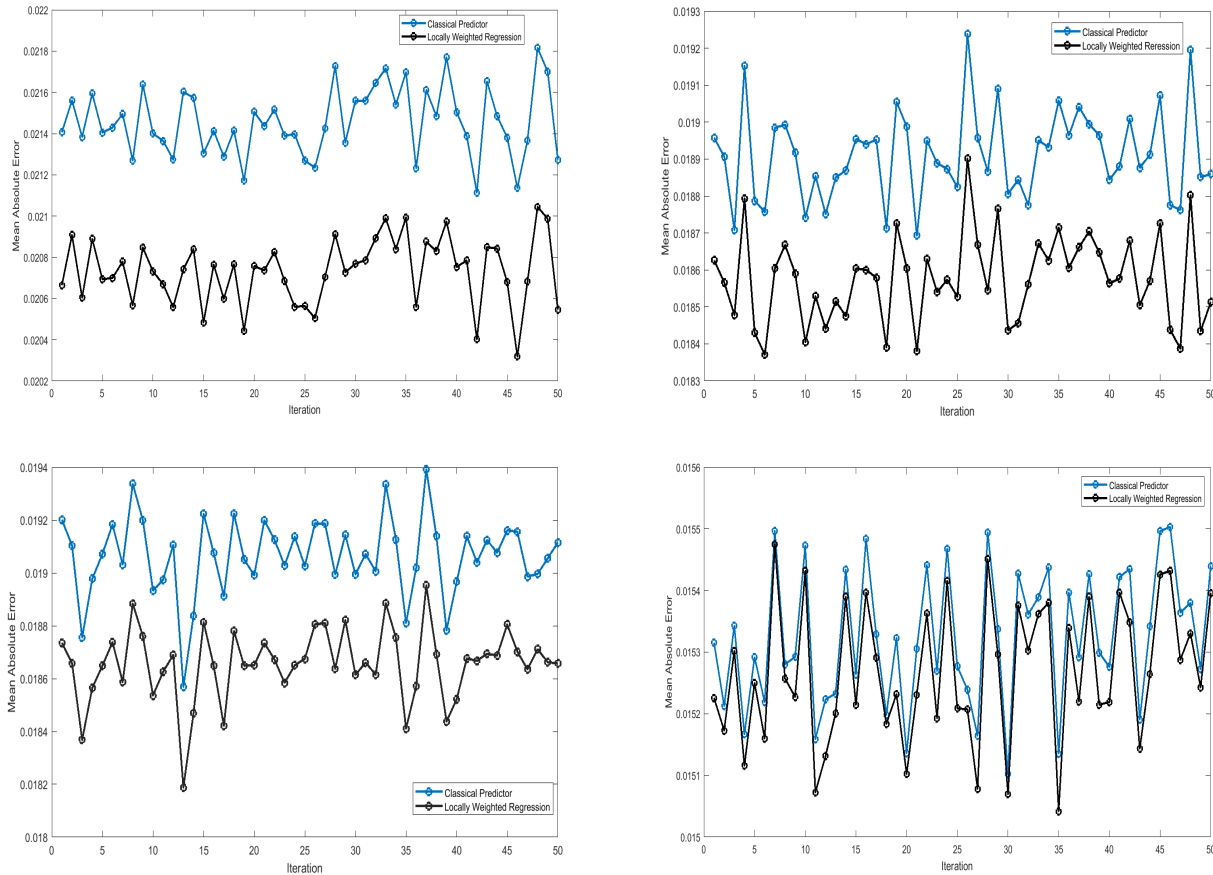


Figure 3: Comparing the classical correlation predictor with the predictor based on Locally Weighted Regression in terms of Mean Absolute Prediction Error for 4 cameras from the Realistic Tampering dataset. From left to right row-wise: a. Canon 60D, b. Nikon D90, c. Nikon D7000 and d. Sony A57.

parameters doesn't necessarily yield an accurate prediction of correlation value. Locally Weighted Regression is a machine learning algorithm which doesn't fit a global set of parameters to a given training set. Instead, it builds a model dynamically based on the query point at which the prediction needs to be made. Thus, the model is built by choosing a linear fit to the training set considering only the points near the vicinity of the query point where we wish to make a prediction. This lets us build a model even for a very nonlinear dataset that follows an arbitrary distribution, with piecewise linear approximations.

Fig. 2 illustrates the idea of Locally Weighted Regression. The dataset shown in the figure is 1-dimensional for the purpose of illustration, but the idea generalizes to any arbitrary dimensions. Consider two query points  $x = 0.55$  and  $x = 1.5$ . The left panel shows least-square regression fit to the dataset of the form:

$$y = \theta_0 + \theta_1 \cdot x$$

where we have a global set of parameters ( $\theta_0$  and  $\theta_1$  in this case). Clearly, if we make predictions based on the global set of parameters, the predictions will not be very accurate. Instead, Locally Weighted Regression considers a subset of training examples from the vicinity of the query point in each case and dynamically builds a model, as illustrated in the figure on the right panel. For instance, for  $x = 0.55$ , it fits the blue line and the predicted

value of  $y$  is given by the  $y$ -coordinate of the cyan point on that line. Similarly, for  $x = 1.5$ , the algorithm fits the red line and the corresponding prediction is again given by the cyan point on that fitted line. Thus, it is a "non-parametric" algorithm in the sense that we don't have a fixed set of parameters of the model that we fit to the training set. Evidently, for both the cases, the prediction is much more accurate than the corresponding predictions obtained by the global linear regression fit (represented respectively by the red and magenta points on the global linear fit).

For Locally Weighted Regression, the cost function that is minimized is defined as:

$$J(\theta) = \sum_{i=1}^m w^{(i)} \cdot (y^{(i)} - \theta^T x^{(i)})^2, \quad (13)$$

which can be minimized with an optimization algorithm such as Gradient Descent. Here  $m$  is the number of training examples,  $y^{(i)}$  is the value of the target variable for the  $i$ -th training example,  $x^{(i)}$  is the corresponding feature vector for the  $i$ -th training example and  $w^{(i)}$  is the weight that is assigned to the  $i$ -th training example. Intuitively, the weights  $w^{(i)}$  are to be assigned very small values for points in the feature space that are far away from the query point. On the contrary,  $w^{(i)}$  should be large for training examples that

are in close vicinity to the query point. There are several choices for the weight function, which is a design choice. One reasonable approach, which is widely used is to define a weight function of the following form:

$$w^{(i)} = \exp\left(-\frac{(x^{(i)} - x)^2}{2\tau^2}\right). \quad (14)$$

The parameter  $\tau$  is known as the "Bandwidth parameter" and determines how sharply the weights fall with distance from the query point. It is evident that if  $x^{(i)}$  lies in the vicinity of the query point  $x$ , then  $w^{(i)}$  will be close to 1 and if  $x^{(i)}$  is far from  $x$  then  $w^{(i)}$  will be close to 0. This implies  $\theta$  is chosen giving a much higher weight to training examples close to the query point  $x$ , ignoring training examples that are far apart. This is shown in Fig. 2 where the algorithm fits two different straight lines respectively at  $x = 0.55$  and  $x = 1.5$ . For the prediction of correlation in PRNU-based manipulation localization,  $x$  is a 4-dimensional feature vector that we choose, representing intensity, texture and flatness characteristics [15], leaving out the quadratic expansion terms involving the 4 features. It is also possible to obtain a closed form solution for the estimate of the parameter vector  $\theta$ , as follows:

$$\hat{\theta} = (H^T W H)^{-1} H^T W \rho, \quad (15)$$

where,  $W$  is an  $m \times m$  diagonal matrix obtained by putting the weights obtained from eq. (14) on the main diagonal. Thus, the  $k$ -th element on the diagonal is the weight of the  $k$ -th training example  $w^{(k)}$ .

## Experimental setup

We work with the Realistic Tampering Dataset [12], which has realistic manipulated images from 4 different digital camera devices which are: Canon 60D, Nikon D90, Nikon D7000 and Sony A57. For each camera, there are 55 genuine uncompressed images and their corresponding manipulated versions. All images are of size  $1080 \times 1920$  pixels. The fingerprint of each camera was estimated from a different set of images. For the correlation predictor with Locally Weighted Regression, we used a total of 110000 genuine image patches of size  $64 \times 64$  as our training examples, for which we had the correlation values and the corresponding 4 features computed for each training example. We compare the accuracy of the standard correlation predictor and the proposed predictor based on Locally Weighted Regression in terms of mean absolute error, defined as:

$$\varepsilon = \frac{1}{N} \sum_{i=1}^N |\rho^{(i)} - \hat{\rho}^{(i)}|, \quad (16)$$

where,  $\rho^{(i)}$  is the true correlation and  $\hat{\rho}^{(i)}$  is the predicted correlation for the  $i$ -th example in the test set and  $N$  is the number of patches in the test set. For manipulation localization, we report the MCC score for manipulation localization masks obtained by our DRF Graph-Cut detector [14], with the two correlation predictors (classical and Lowess-based). The MCC score is defined as:

$$MCC = \frac{TP \times TN - FP \times FN}{\sqrt{(TP + FP)(TP + FN)(TN + FP)(TN + FN)}}, \quad (17)$$

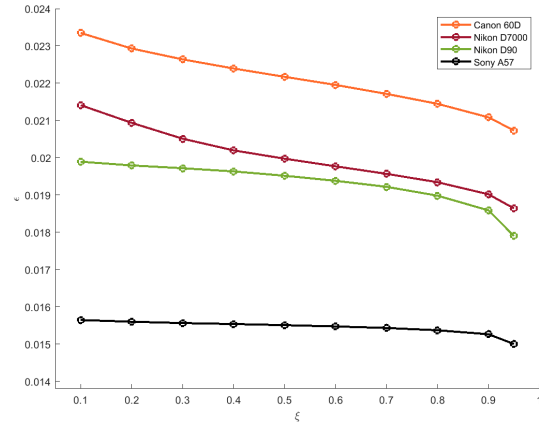


Figure 4: A typical plot of  $\varepsilon$  vs.  $\xi$  (based on Realistic Tampering dataset).

where, TP, TN, FP and FN respectively represents the number of True Positive, True Negatives, False Positives and False Negatives.

## Results

Fig. 3 shows the comparison of the classical correlation predictor and the proposed predictor based on Locally Weighted Regression (Lowess) in terms of eq. (16), for the 4 cameras from the Realistic Tampering dataset [12]. Here, for each camera, we used a training set consisting of 110000 patches of size  $64 \times 64$  and the corresponding correlation values, to fit the locally weighted regression while making the prediction on the test set. The test dataset consists of 110000 patches which are disjoint from the training patches. For each camera, we randomly sample 10000 patches from the test set and make prediction of correlation by the two predictor, repeating the process for 50 iterations (i.e., we randomly sampled the test set 50 times and compared the performance of the two predictors in each iteration). The predictor based on Lowess was obtained by dynamically fitting the model on examples from the training set, which are disjoint from the test set. We observe that the proposed predictor based on Lowess clearly outperforms the classical predictor by a fair margin, as it consistently yields a lower prediction error for all 4 cameras. However, since the predictor is based on a model that is fit dynamically to the training set as per eq. (15), for every pixel in a query image at which we need to make a prediction, this appears to be computationally more expensive than the global fit to the training set. Indeed, the diagonal matrix  $W$  in eq. (15) will be very large if we have a very large training set and hence it is an expensive algorithm to fit when the training set is very large. However, it can be implemented very efficiently even for large datasets with millions of training examples using algorithms like k-d trees for instance [18]. We used a different approach to fit the model efficiently, without having the need to formulate the diagonal matrix. Instead of setting the bandwidth parameter  $\tau$ , we select a threshold  $\xi$  for the weights for each camera and considered all the points near the vicinity of the query point for which the value of weight is above the threshold  $\xi$ . We experimented different values of  $\xi$  and chose the value of  $\xi$  as 0.95 for each camera. Indeed, this approach has the same effect of choosing the points near the vicinity of the query point by varying

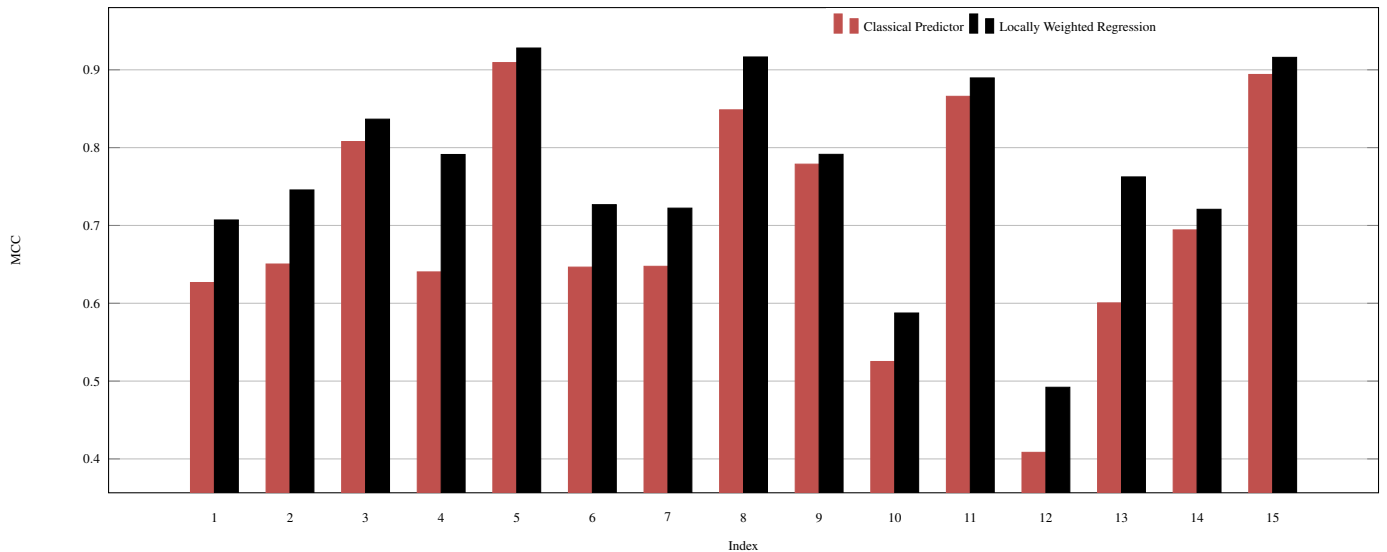


Figure 5: Manipulation localization performance in terms of MCC score comparing the classical predictor and the proposed predictor based on Lowess, based on Realistic Tampering dataset.

the bandwidth parameter  $\tau$ . We kept the parameter  $\tau$  fixed at 0.05. Fig. 4 shows how the value of  $\varepsilon$  in eq.(16) varies as a function of  $\xi$ . We observe that the value of  $\varepsilon$  steadily decreases as we increase the value of  $\xi$ , which corresponds to considering points nearer and nearer to the vicinity of the query point  $x$ . With this approach, the model can be implemented very efficiently with vectorized code.

Fig. 5 shows the comparison of manipulation localization results obtained when we incorporated the proposed predictor, as well as the classical predictor with our DRF GraphCut detector [14]. The MCC score obtained on some manipulated images from Realistic Tampering dataset for the same operating threshold settings ( $\eta = 0.025$ ,  $\tau = 0.04$ ) for the two detectors has been shown, which reveals that the proposed correlation predictor yields a better manipulation localization performance than the classical predictor. We also show some manipulation localization masks generated by our detector when combined with the proposed correlation predictor.

## Conclusion

We propose a correlation predictor for PRNU-based image manipulation localization based on a non-parametric algorithm, which is Locally Weighted Regression (Lowess). Instead of fitting a global set of parameters  $\theta$  to a quadratic model involving the 4 features representing the intensity, texture and flatness characteristics, the proposed predictor based on Lowess fits a model dynamically considering training examples lying in the vicinity of the query point in the feature space. Thus, while building the predictor, we consider only the image patches from the training set that have similar intensity, texture and flatness characteristics measured by the 4 fundamental features as described before. This algorithm allows us to fit a model very effectively even for a very non-linear function with piece-wise linear approximations. Our experimental results indicate that the proposed correlation predictor yields a better accuracy of predicting correlations than the classical predictor that is based on a global set of parameters. Although, for large training sets, the algorithm is computationally

more expensive than a global fit to the entire training set, it can be implemented very efficiently using k-d trees even when the training set is very large. Our manipulation localization results as well as the low prediction errors based on Realistic Tampering dataset [12] indicate the efficacy of the proposed correlation predictor.

## References

- [1] R. Böhme and M. Kirchner, "Media forensics," in *Information Hiding*, S. Katzenbeisser and F. Petitcolas, Eds. Artech House, 2016, ch. 9, pp. 231–259.
- [2] J. Lukas, J. Fridrich, and M. Goljan, "Digital camera identification from sensor pattern noise," *IEEE Transactions on Information Forensics and Security*, vol. 1, no. 2, pp. 205–214, 2006.
- [3] J. Fridrich, "Sensor defects in digital image forensics," in *Digital Image Forensics: There is More to a Picture Than Meets the Eye*, H. T. Sencar and N. Memon, Eds. Springer, 2013, pp. 179–218.
- [4] M. Chen, J. Fridrich, and M. Goljan, "Source digital camcorder identification using ccd photo response nonuniformity," in Proc. SPIE, Electronic Imaging, Security, Steganography, and Watermarking of Multimedia Contents IX, E. Delp and P. Wong, Eds., vol. 6505, January 2007, pp. 1G 1–12.
- [5] T. Filler, J. Fridrich, and M. Goljan, "Using sensor pattern noise for camera model identification," in Proc. ICIP 2008, San Diego, CA, October 12-15 2008, pp. 1296–1299.
- [6] M. Goljan, "Digital camera identification from images—Estimating false acceptance probability," in Proc. 7th Int. Workshop Digital Watermarking, Busan, Korea, Nov. 10–12, 2008.
- [7] M. Goljan and J. Fridrich, "Camera identification from scaled and cropped images," in Proceedings of SPIE, Electronic Imaging, Security, Forensics, Steganography, and Watermarking of Multimedia Contents X, E. J. D. et al., Ed., vol. 6819. San Francisco, CA: SPIE, January 2008, pp. 0E 1–13.
- [8] M. Goljan and J. Fridrich, "Sensor-fingerprint based identification of images corrected for lens distortion," in Proceedings of SPIE, Electronic Imaging, Media Watermarking, Security, and Forensics 2012, N. Memon, A. Alattar, and E. D. III, Eds., vol. 8303, San Francisco,

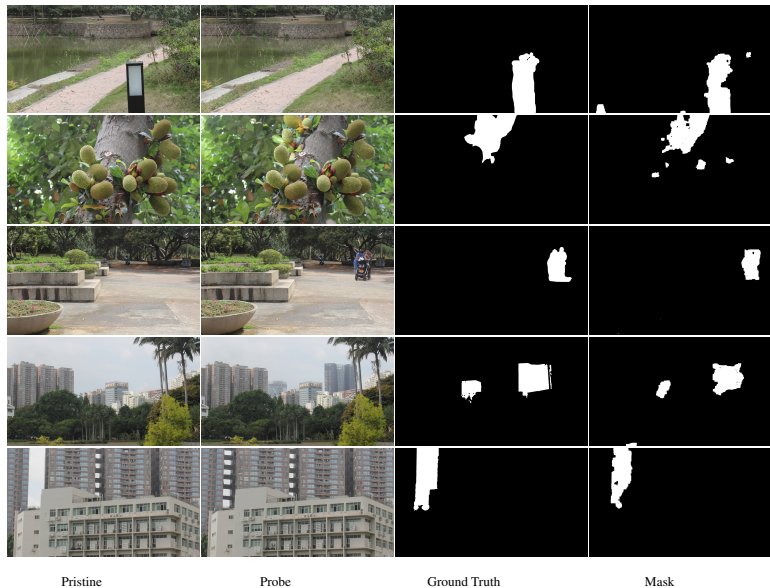


Figure 6: Localization results with the proposed correlation predictor. From left to right: Original image; manipulated image; ground truth and mask generated with the DRF GraphCut detector incorporating the proposed predictor.

- CA, January 2012, pp. 0H 1–13.
- [9] M. Goljan, J. Fridrich, and M. Chen, “Sensor noise camera identification: Countering counter-forensics,” in Proc. SPIE Electronic Imaging, Steganography, Security, and Watermarking of Multimedia Contents XII, N. Memon, J. Dittmann, A. Alattar, and E. Delp, Eds., vol. 7541, January 17–21, 2010, pp. 0S 1–12.
- [10] M. Goljan, J. Fridrich, and T. Filler, “Large scale test of sensor fingerprint camera identification,” in Proc. SPIE, San Jose, CA, Jan. 18–22, 2009, vol. 7254, pp. 0I 1–0I 12, Electronic Imaging, Media Forensics and Security XI.
- [11] G. Chierchia, G. Poggi, C. Sansone, and L. Verdoliva, “A Bayesian-MRF approach for PRNU-based image forgery detection,” *IEEE Transactions on Information Forensics and Security*, vol. 9, no. 4, pp. 554–567, 2014.
- [12] P. Korus and J. Huang, “Multi-scale analysis strategies in PRNU-based tampering localization,” *IEEE Transactions on Information Forensics and Security*, vol. 12, no. 4, pp. 809–824.
- [13] S. Chakraborty and M. Kirchner. PRNU-based image manipulation localization with discriminative random fields. *Electronic Imaging*, 2017(7):113–120, 2017.
- [14] S. Chakraborty and M. Kirchner. Sensor-based image manipulation localization with discriminative random fields and Graph Cut. *Journal of Visual Communication and Image Representation*, Volume 80, October 2021.
- [15] M. Chen, J. Fridrich, M. Goljan, and J. Lukáš, “Determining image origin and integrity using sensor noise,” *IEEE Transactions on Information Forensics and Security*, vol. 3, no. 1, pp. 74–90, 2008.
- [16] S. Chakraborty. A CNN-Based Correlation Predictor for PRNU-Based Image Manipulation Localization. *Electronic Imaging*, 2020(7):pp. 78-1-78-8(8), 2020.
- [17] T. Gloe, S. Pfennig, and M. Kirchner, “Unexpected artefacts in PRNU-based camera identification: A ‘Dresden Image Database’ case-study,” in *ACM Multimedia and Security Workshop (MM&Sec)*, 2012, pp. 109–114.
- [18] Andrew Moore, Jeff Schneider and Kan Deng, “Efficient Locally Weighted Polynomial Regression Predictions”, in Proceedings of

(ICML) International Conference on Machine Learning, July 1997, pp. 236–244.

## Author Biography

*Sujoy Chakraborty received his ME in Software Engineering from Jadavpur University, Kolkata (2008), India and his PhD in Electrical and Computer Engineering from the State University of New York, Binghamton (2019). He is currently working as an Assistant Professor of Computer Science at Stockton University, NJ. His work has focused primarily on digital image forensic techniques based on digital camera sensor noise, application of deep learning on sensor-based image forensics, as well as algorithms based on compression forensics and counter forensics.*

*Erick Garcia-Vargas received his BS in Computer Science from Stockton University (2021). He is currently employed by QualIT Innovation Solution LLC. His current research interests are at the intersection of Healthcare and Machine learning.*